Temperature Dependence of Water Dynamics in Poly(Ethylene Oxide)/Water Solutions from Molecular Dynamics Simulations and Quasielastic Neutron Scattering Experiments

ARTICLE *in* THE JOURNAL OF PHYSICAL CHEMISTRY B · APRIL 2002

Impact Factor: 3.3 · DOI: 10.1021/jp0200021

4 AUTHORS, INCLUDING:

Oleg Borodin
Army Research Laboratory
182 PUBLICATIONS **4,125** CITATIONS
SEE PROFILE

Dmitry Bedrov
University of Utah
164 PUBLICATIONS **3,151** CITATIONS
SEE PROFILE

Temperature Dependence of Water Dynamics in Poly(Ethylene Oxide)/Water Solutions from Molecular Dynamics Simulations and Quasielastic Neutron Scattering Experiments

Oleg Borodin,*,† Frans Trouw,‡ Dmitry Bedrov,† and Grant D. Smith†

Department of Materials Science and Engineering and Department of Chemical and Fuels Engineering, 122 S. Central Campus Dr., Rm. 304, University of Utah, Salt Lake City, Utah 84112, and Manuel Lujan Jr., Neutron Scattering Center, MS H805, Los Alamos National Laboratory, New Mexico 87545

Received: January 7, 2002

The dynamics of water in aqueous solutions of poly(ethylene oxide) (PEO) were studied by performing molecular dynamics (MD) simulations and quasielastic neutron scattering (QNS). The simulations and experiments were carried out on PEO/water solutions for the composition EO:O_w (ether oxygen:water oxygen) = 1:2.3 in the temperature range from 298 to 410 K. To selectively measure the motion of the water, perdeuterated PEO (d-PEO) was used for the QNS experiments. Intermediate scattering functions derived from the MD simulations were found to be in good agreement with those from QNS experiments. The QNS and MD dynamic structure factors were analyzed using the random jump diffusion (RJD) model, a model frequently applied in analysis of water QNS data, yielding rotational and translational diffusion coefficients for water in the d-PEO/H_2O solutions. Analysis of MD results indicates that, although the translational self-diffusion coefficient can be extracted from the RJD fits to the data rather accurately, the rotational diffusion coefficient has an uncertainty of a factor of 3. The water rotational relaxation was found to be anisotropic, with the rotation in the plane perpendicular to the water dipole vector being 2−2.5 times faster than the water dipole vector relaxation. The Sears model of isotropic rotation provided a poor description of the water rotational dynamics at 298 and 368 K, with better agreement at 410 K. The increased anisotropy of water rotation in PEO/water solutions compared to that of pure water is attributed to PEO/water electrostatic interactions.

I. Introduction

Poly(ethylene oxide) (PEO) has a wide range of technologically important applications. For example, grafting of PEO on the surface or adsorption of PEO-poly(propylene oxide)-PEO block copolymers (Pluronic) prevents protein adsorption and denaturation thus making surfaces more biocompatible.[1−6] Lightly cross-linked PEO is the main constituent of many hydrogels used for drug delivery applications.[7] Attaching PEO to proteins prevents them from being adsorbed on surfaces,[3] whereas aqueous solutions of PEO with dextran, starch, and poly(vinyl alcohol) are used for industrial protein partitioning.[3] Because of the widespread importance of PEO in aqueous solutions, we[8−16] and other groups[17−21] have conducted molecular dynamics (MD) simulation studies of ether/water and PEO/water solutions in order to gain atomistic level insight into the thermodynamic structured and dynamic properties of PEO and its oligomers in aqueous solution. We demonstrated the ability of MD simulations using our quantum-chemistry based force field[8,22] to accurately predict water self-diffusion coefficients,[11,14,22] excess volume[8,22] and changes in 1,2-dimethoxyethane (DME) conformations[9] with composition in DME/water solutions, free energy, and enthalpy of DME hydration.[22] More recently we have utilized MD simulations to look at the conformations[15] and hydrogen bonding[16] in PEO/water solutions. In the following paper of this issue, we explore concentration dependence of water dynamics.

In this contribution, we report the results of a coordinated MD simulation and quasielastic neutron scattering (QNS) study of water dynamics in aqueous solutions of PEO (M_w = 2378 in MD and M_w = 2300 in QNS) at a composition of (ether oxygen):(water oxygen) = 1:2.3. This composition corresponds to a polymer weight and volume fraction of about 0.5, at which the majority of water molecules are located in the first coordination shell of PEO chains; that is, practically all water is interfacial water, and no free water exists in the solutions.[16] In this paper, we focus on comparing water dynamics from MD simulations with that from QNS experiments for the purpose of gaining a better understanding of the influence of PEO−water interactions on water dynamics. An additional and related question addressed here is the applicability of a widely used random jump diffusion (RJD) model for water dynamics in the analysis of QNS spectra of aqueous solutions.

The present QNS study is different from the previous studies of PEO/water solutions.[23−25] We use fully deuterated PEO (d-PEO) with hydrogenated water, as the large incoherent neutron scattering cross-section of hydrogen (the neutron scattering cross-section of deuterium is a factor of 16 smaller than that of water) allowed us to focus on the scattering from the water. This simplifies the interpretation of the water dynamics compared with the previous experiments on hydrogenated PEO/water solutions.[24,25] This QNS study (with energy resolution about 100 μeV) explores much faster water dynamics than the previous QNS study of d-PEO/water solutions by Barnes et al.[23] done on the IN10 backscattering spectrometer at the ILL (energy resolution approximately 1 μeV). Furthermore, the temperature dependence of the water dynamics and a detailed comparison to the results of the MD simulations were not a part of the

* To whom correspondence should be addressed. E-mail: borodin@eng.utah.edu.
† University of Utah.
‡ Los Alamos National Laboratory.

10.1021/jp0200021 CCC: $22.00
Published on Web 04/30/2002

previously published QNS studies. The outline of the paper is the following: In section II, we briefly describe the methodology of the QNS experiments and MD simulations, followed by the direct comparison of the intermediate scattering functions from QNS experiments and MD simulations in section III. In section IV, we discuss the RJD model for water dynamics and apply it to the analysis of QNS data. In sections V and VI the temperature dependence of water rotational and translational dynamics from MD simulations is discussed in detail. The validity of the main assumptions of the RJD model for water dynamics is also investigated in sections V and VI by comparing separately rotational and translational contributions to water motion from MD simulations with the functional form postulated in the jump diffusion model. Finally, water rotational and translational dynamics in bulk water is compared to that in PEO/water solutions in section VII.

II. Experimental and Simulation Methodology

Quasielastic Neutron Scattering Experiments. The experiments were carried out at the Intense Pulse Neutron Source division of the Argonne National Laboratory using the QNS spectrometer,[26] a "crystal-analyzer", or "inverse-geometry" spectrometer that accepts a white beam from the solid methane moderator onto the sample. Constant-energy focusing of the graphite analyzer crystal arrays provides resolution of $\sim 100\ \mu$eV for the quasielastic and low-energy inelastic scattering. The complete scan using the rotating table yields nine spectra covering the momentum transfer range from 0.5 to 2.5 Å^{-1}.

D-PEO ($M_w = 2300$, $M_n/M_w = 1.2$) was purchased from MSD (Quebec, Canada) and was used without further purification. After d-PEO was added to the purified H_2O, samples were shaken for 4−6 h in order to ensure proper mixing. The samples were evenly distributed in a cylindrical aluminum envelope to minimize sample thickness and thus reduce multiple scattering and placed in a circular thin aluminum cylinder approximately 12 cm long and 0.7 cm in diameter. The sample was kept in the container using an indium gasket seal as the sample is placed in a vacuum during the experiment. Experiments were performed at a PEO concentration of EO:O_w = 1:2.3 and temperatures of 298, 368, and 410 K. Measurement of the QNS spectra of the neat d-PEO at 298 K was also performed. Typical data collection time was 6−8 h. The time-of-flight data were then transformed into the neutron scattering law, S(Q,ω), using the standard conversion programs.

Molecular Dynamics Simulations. MD simulations were performed on CH_3-capped 54 repeat unit PEO chains (M_W = 2378) in water at a concentration corresponding to EO:O_w = 1:2.3 and also for pure water. The simulated ensemble for the aqueous solution of PEO consisted of the 620 water molecules and 5 PEO chains, whereas 500 water molecules were used in pure water simulations. Simulations were performed at 298 K, 318, 368, and 410 K. Explicit atom quantum chemistry based PEO/PEO[27] and PEO/water[22] force fields together with the TIP4P water model[28] were used. The PEO/water system was created by inserting polymer chains and water molecules in a cubic box with a linear dimension of 65 Å. The box was shrunk in MD simulations using a Brownian dynamics algorithm[29] for 1.5 ns to 35 Å^3. Then the system was equilibrated at 450 K for 500 ps using the Brownian dynamics algorithm in order to facilitate mixing and for 1 ns using velocity Verlet algorithm with a 1 fs time step.[30] At each temperature, 1 ns constant pressure runs at 1 atm were performed in order to determine the equilibrium solution density. Subsequent sampling runs in an NVT ensemble were 2−8 ns for PEO/water solutions. For pure water, 750 ps production runs were performed in an NVT ensemble corresponding to the water density at 1 atm obtained from 300 ps runs in an NPT ensemble. The Nose−Hoover thermostat[31] and barostat[32] were used to control temperature and pressure. Bond lengths were constrained using the Shake algorithm.[33] The Ewald summation method[34] was used for treatment of long-range electrostatic forces. A multiple time step reversible reference system propagator algorithm with three time steps was employed:[32] a time step of 0.7 fs for bonding, bending, and torsional motions, a 1.4 fs time step for nonbonded interactions within a 6.5 Å sphere, and a 2.8 fs time step for nonbonded interactions between 6.5 and 10.0 Å and the reciprocal space part of the Ewald summation.

III. Intermediate Scattering Function for d-PEO/H_2O Solutions

We begin data analysis by making a direct comparison of water dynamics in PEO/water solutions from QNS experiments and MD simulations. The most direct comparison between experiment and simulation is achieved by comparing the intermediate scattering functions $I(Q,t)$ (ISFs) measured in the QNS experiment to those calculated from the simulations. As the scattering from hydrogen is the dominant contribution, and it is essentially entirely incoherent scattering, only the incoherent ISF is relevant. For isotropic systems such as liquids, the incoherent ISF is given by[35]

$$I_{inc}(Q,t) = \left\langle \frac{\sin(\Delta r_i(t)Q)}{\Delta r_i(t)Q} \right\rangle \qquad (1)$$

where $\Delta r_i(t)$ is the displacement of atom i after time t, Q is the magnitude of the momentum transfer vector, and $\langle\ \rangle$ denotes an average over all time origins and atoms with significant incoherent cross-section (water hydrogen atoms). The ISFs from MD simulations were calculated using eq 1, whereas the Fourier transformation of the experimentally measured $S(Q,\omega)$ from the frequency domain into time domain is required in order to obtain the ISFs from QNS measurements. Several issues arise during the Fourier transformation affecting the resulting $I(Q,t)$, namely, the effect of truncation after 1.5 meV in the frequency domain, the effect of the experimental background, residual elastic scattering, and the effect of the Debye−Waller factor and the resolution function. These issues have been recently discussed by us in ref 9 Appendix A. In the current work, the experimental background and the scattering that is due to the empty can were subtracted from $S(Q,\omega)$ prior to Fourier transformation, but no correction was made for the small contribution of d-PEO scattering, as explained below.

The ISFs for water in PEO/water solutions at 298, 368, and 410 K from MD simulations and QNS experiments are shown in Figure 1a−c for a number of Q values covering the experimentally accessible range. For all temperatures, the ISFs from MD simulations agree quite well with those from the QNS experiments for Q values below 1.0 Å^{-1}. For higher Q values, MD simulations predict faster decay of $I(Q,t)$ than QNS experiments. At 298 K, the slopes of $I(Q,t)$ from MD simulations and QNS experiments are clearly similar for high Q values, whereas similarity between the slopes of $I(Q,t)$ from MD and QNS at 368 and 410 K are less pronounced because of high scattering of experimental data. Indeed, MD simulations at 368 and 410 K indicate that water molecules are rotating at a rate such that the decay has reduced the ISF to approximately 0.2−0.3 within the first picosecond. The characteristic observation time of the spectrometer is up to about 40 ps (determined by

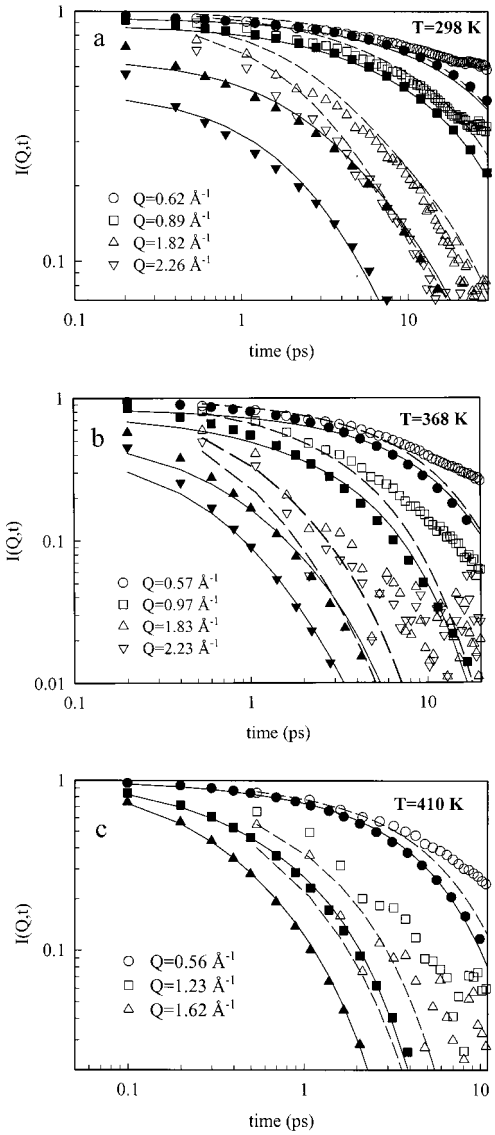

Figure 1. Water intermediate scattering functions from the Fourier transform of $S(Q,\omega)$ QNS data (open symbols), MD simulations (closed symbols), the RJD model approximation of QNS data in $S(Q,\omega)$ space (dashed line), and the RJD model fits to MD data (solid line) for 298 (a), 368 (b), and 410 K (c).

the energy resolution). This mismatch between the energy resolution of the spectrometer and the decay of the ISF results in the large scatter in the data for the larger momentum transfers and temperatures. In other words, the components are very broad in $S(Q,\omega)$ compared with the resolution of the spectrometer, and a spectrometer with a reduced energy resolution and a concomitant increase in count-rate is needed to obtain better data under those conditions. Nevertheless, the measured and predicted decays are in reasonable agreement for 368 and 410 K. The flattening out of the ISFs derived from the measured $S(Q,\omega)$ is a consequence of the scattering from the d-PEO and is sufficiently small that it can be ignored (i.e., the d-PEO gives rise to some coherent elastic scattering which results in a small but finite asymptotic limit in the decay of the ISF).

In summary, general agreement between ISFs from MD simulations and QNS experiments for the PEO/water solutions is acceptable, especially at low Q values, indicating that the force field used in MD simulation is capable of predicting water proton motion in PEO/water solutions on the time scale 0.5−30 ps reasonably well. We note that good agreement between MD simulations and QNS experiments was also seen at the same composition (EO:O_W = 1:2.3) for water diffusion in dimethoxyethane (DME = H−$(CH_2OCH_2)_2$−H) aqueous solutions at 318 K.[14,22]

IV. Random Jump-Diffusion Model

The RJD model has been successfully applied to the analysis of QNS spectra obtained for water motion in pure water,[36] DME/water[9,14] and on the surface of globular proteins.[37] This model yields the water translational and rotational diffusion coefficients from QNS data through fitting of the $S(Q,\omega)$ spectra. Below, we briefly describe the formalism of the RJD model in the time domain and apply it in analysis of the $S(Q,\omega)$ spectra in the frequency domain for the aqueous solution of d-PEO measured on QNS. Conversion of the RJD model from time to frequency domain is done by numerical inverse Fourier transform taking into account the effect of the resolution function and the relative efficiency of the instrument.

Description of the RJD Model. In the RJD model, water molecules undergo two types of motion: a local oscillatory motion in a cage for a mean residence time τ_0 followed by an instantaneous jump of mean length l_{jump} to a new "cage". Following Singwi and Sjölander[38] and Teixeira et al.,[36] who assumed no coupling of rotation and translational motion, the intermediate scattering function is given by:

$$I(Q,t) = \mathrm{DW}(Q)\, T(Q,t)\, R(Q,t) \tag{2}$$

where DW(Q) is the Debye−Waller factor which takes into account vibrational motion of atoms, $T(Q,t)$ describes translational motion of water, and $R(Q,t)$ describes rotational motion. The rotational motion is represented by the first three terms of the well-known expansion of the classical rotational diffusion of a water molecule due to Sears.[39] The translational contribution $T(Q,t)$ of water was found by Singwi and Sjölander[38] and Teixeira et al.[36] to be adequately described by

$$T(Q,t) = \exp[-\Gamma(Q)t] \tag{3}$$

where $\Gamma(Q)$ is the line width of the translational component of the spectrum and is described in the RJD model by[36,38]

$$\Gamma(q) = \frac{DQ^2}{1 + DQ^2\tau_0} \tag{4}$$

where the translational diffusion coefficient D is given in terms of the above-mentioned mean-square jump length l_{jump}^2 and mean-residence time τ_0

$$D = \frac{l_{\mathrm{jump}}^{\ 2}}{6\tau_0} \tag{5}$$

Rotational diffusion is represented by the first three terms of the expansion due to Sears[39]

$$R(Q,t) = j_0^{\,2}(Q,a) + 3j_1^{\,2}(Q,a)\exp(-t/(3\tau_{\mathrm{rot}})) + 5j_2^{\,2}(Q,a)\exp(-t/\tau_{\mathrm{rot}}) \tag{6}$$

where $j_n(Q,a)$ are spherical Bessel functions of the order n, τ_{rot} is the water rotational relaxation time, and a is the radius of the sphere on which the motion of water protons occurs. Following our previous work,[9] we used a = 0.92 Å.

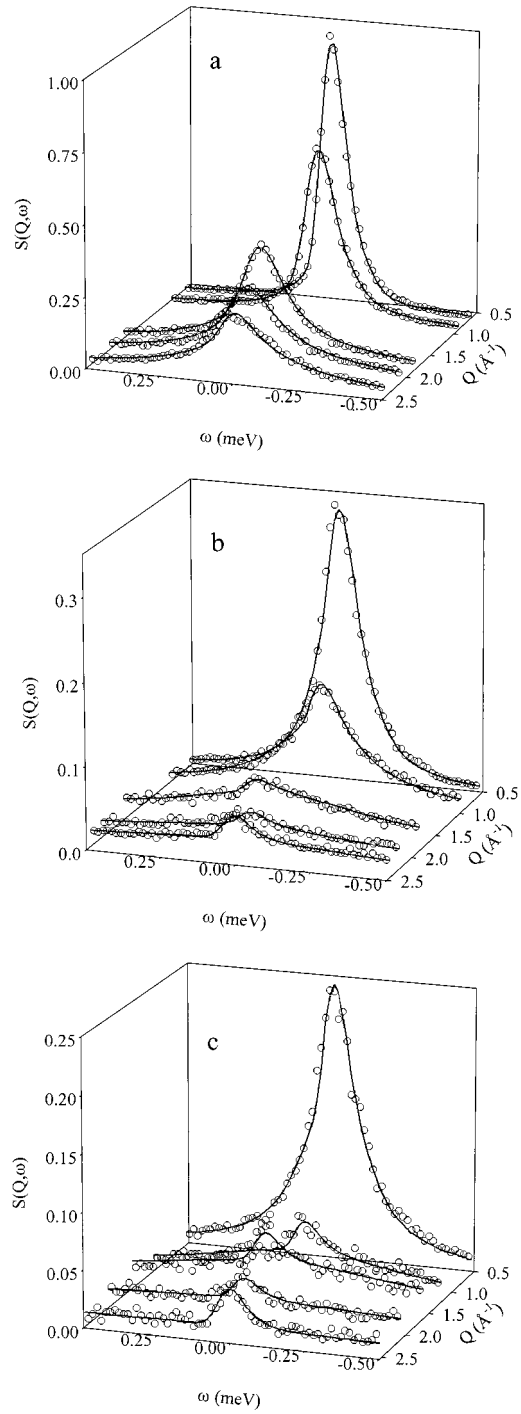

Figure 2. Dynamic structure factor $S(Q,\omega)$ from QNS measurements (open symbols) and fits by the RJD model (lines) for 298 (a), 368 (b), and 410 K (c).

Analysis of QNS Data For d-PEO/H_2O Solutions Using the RJD Model. $S(Q,\omega)$ spectra from QNS experiments contain contributions from water, d-PEO, and scattering from the aluminum can. Scattering due to the empty can was subtracted from the $S(Q,\omega)$ data. It is desirable to subtract the small contribution to the total $S(Q,\omega)$ that was due to scattering from d-PEO. This, however, cannot be achieved by subtracting $S(Q,\omega)$ of pure d-PEO melts, as PEO dynamics in the melt and in aqueous solutions are significantly different.[12] To account for the contribution from d-PEO scattering, an extra delta function was added during fitting of the $S(Q,\omega)$ spectra for all temperatures as was previously done in the analysis of DME/water[14] and globular protein[37] QNS spectra.

TABLE 1: Water Rotational Relaxation Time (τ_{rot}), Mean Jump Length (l_{jump}), Mean Residence Time (τ_0), and Water Self-Diffusion (D_W) from the RJD Fit to the QNS Data and MD Simulations

		parameters of the RJD model				
T (K)	fitted data	l_{jump} (Å)	τ_0 (ps)	τ_{rot} (ps)	D_W (Å²/ps)	D_W from MSD (Å²/ps)
298	$S(Q,\omega)$, QNS	3.42	16.4	1.33	0.12	
	$I(Q,t)$, MD	2.48	11.4	1.35	0.091	0.064
	$I_{cm}(Q,t)$, MD	1.57	6.27		0.065	
	$I_{rot}(Q,t)$, MD			4.99		
	$I(Q,t)$, MD τ_{rot}=4.99 ps[a]	1.15	3.75	4.99[a]	0.059	
368	$S(Q,\omega)$, QNS	1.60	1.18	0.36	0.36	
	$I(Q,t)$, MD	1.17	0.59	0.17	0.39	0.372
	$I_{cm}(Q,t)$, MD	1.25	1.73		0.40	
	$I_{rot}(Q,t)$, MD			0.70		
410	$S(Q,\omega)$, QNS	1.50	0.63	0.32	0.60	
	$I(Q,t)$, MD	1.07	0.31	0.14	0.61	0.683
	$I_{cm}(Q,t)$, MD	0.95	0.25		0.60	
	$I_{rot}(Q,t)$, MD			0.37		

[a] τ_{rot} was constrained to 4.99 ps, whereas the other parameters were allowed to vary.

The experimental $S(Q,\omega)$ spectra for nine momentum transfers from 0.5 to 2.6 Å^{-1} were simultaneously fitted for energy transfers from −1.5 to +3 meV with the same set of parameters (l_{jump}, τ_0, τ_{rot}) for each temperature, but the magnitudes of the extra delta functions for the Q-dependent d-PEO scattering were allowed to independently vary for each spectra. The Debye−Waller factor was allowed to vary for each sample. The resulting values of the Debye−Waller factor were in the range of 0.54−0.67 similar to the value of 0.484 determined by Teixeira et al.[36] for pure water. We also found that the fits were relatively insensitive to contributions due to water rotation in agreement with Ullo's[40] conclusions from MD analysis of water QNS spectra. Consequently, the rotational diffusion constants obtained by fitting of the RJD model to the experimental data have larger error bars than the translational self-diffusion coefficient. The dynamic structure factors $S(Q,\omega)$ from QNS measurements together with the resulting RJD model fits for the d-PEO/H_2O are shown in Figure 2a−c. The RJD model is able to fit QNS data well for the measured range of momentum transfers with small deviations of the fits from the experimental data observed only for the smallest Q values. The l_{jump}, τ_0, and τ_{rot} parameters are summarized in Table 1. The mean jump length (l_{jump}), mean-residence time (τ_0), and rotational relaxation time (τ_{rot}) were found to decrease with increasing temperature, in accord with the results of Teixeira et al.[36] for pure water measured at temperatures from 253 to 298 K. At 298 K a mean-jump length of 3.42 Å for water diffusion in PEO/water solutions is larger than that for pure water[36] (1.29 Å), whereas the average residence time of water molecules in PEO/water solutions (16.4 ps) is an order of magnitude larger than that for pure water (1.25 ps). The RJD model yields a water self-diffusion coefficient in d-PEO/water solutions at 298 K of 0.12 Å²/ps, which is two times smaller than that of pure water.[36]

To confirm that the extra delta functions used in the RJD fits indeed represent coherent contribution of PEO scattering, we have compared in Figure 3 the intensities of the extra delta function for each spectrum from RJD fits to QNS data with the contribution of d-PEO to the total structure factor $S(Q)$ of d-PEO/H_2O solutions as obtained from MD simulations given by eq 7:

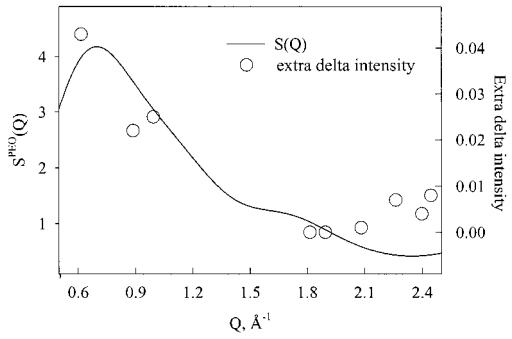

Figure 3. Coherent static structure factor for d-PEO in PEO/water solutions from MD simulations and extra delta intensity from RJD model fits for QNS data at 298 K.

$$S(Q) = 1 + n\sum_{\alpha\beta} x_\alpha b_\alpha x_\beta b^*_\beta \int_0^\infty [g_{\alpha\beta}(r) - 1]\frac{\sin Qr}{Qr} 4\pi r^2 \, dr \tag{7}$$

where x_α denotes the number concentration of species α, b_α is the scattering length for the species α, $g_{\alpha\beta}(r)$ is the radial distribution function for species α and β, and n is the total number density. Only contributions from d-PEO to $S(Q)$ were taken into account, and water was excluded from the summation in eq 7.

The most significant extra delta function scattering (obtained from the fits) is in the first three spectra (Q = 0.62, 0.89, 0.99 Å^{-1}) where the extra delta function represents about $^1/_3$, $^1/_6$, and $^1/_6$ of the scattering respectively at 298 K. For the rest of the Q values, the extra delta function is less than 5% of the scattering. This is consistent with the large peak in the polymer $S(Q)$ at these lower Q values. At the higher temperatures, the extra delta function contribution is further reduced by about a factor of 2 relative to the RJD model scattering at 298 K. Therefore, we conclude that the extra delta function intensities from RJD model fits to QNS data indeed represent coherent scattering of d-PEO, as assumed.

It is also instructive to compare ISFs obtained from Fourier transform of the RJD model fits to the experimental $S(Q,\omega)$ with the ISFs obtained by Fourier transform of the experimental data. Figure 1a−c shows such a comparison for 298, 368, and 410 K, respectively. At 298 K, the long time behavior of ISFs obtained from the RJD model agrees well with the experimental ISFs for large momentum transfers for times longer than 3−5 ps. Deviation of the RJD model from the direct Fourier transform data for short times (t < 5 ps) is attributed to inability of RJD model to correctly describe water rotation on a picosecond time scale in PEO/water and will be discussed below. For small momentum transfers (Q < 1 Å^{-1}), ISFs obtained by Fourier transform of QNS data decay systematically slower for all temperatures than those from RJD fits to QNS data because of residual elastic scattering, which was effectively removed from the RJD model by adding an extra delta function in the fitting of $S(Q,\omega)$ by the RDJ model. Figure 1a−c also shows that the ISFs from the RJD model generally agree better with ISFs from MD simulations than those obtained directly from the experimental $S(Q,\omega)$ by Fourier transform because of the removal of noise and elastic scattering of d-PEO during fits to the RJD model.

RJD Model Analysis of the MD Simulations Data For d-PEO/H_2O Solutions. As the RJD model is capable of describing QNS data shown in Figure 2, it is also expected to describe ISFs from MD simulations. We found that the quality of the fits improves if a preexponential Q dependent amplitude is used in eq 3. This amplitude was found to decrease linearly with increasing Q, as was previously discussed by us[9] and shown in Figure 4a in ref 9. The Q dependence of this amplitude was also shown to mimic the Debye−Waller factor.[9] By including this amplitude in the fits, we ignore the fast subpicosecond water relaxation process, which yields a very insignificant contribution to the $S(Q,\omega)$ for Q < 2.5 Å^{-1}. RJD model fits to MD data are shown in Figure 1 over the time scale of 0.5−30 ps corresponding to the experimentally accessible time scale, indicating that that the RJD model fits the $I(Q,t)$ data well. The resulting parameters of the RJD model are given in Table 1. Table 1 shows that the self-diffusion coefficient obtained by fitting RJD model to MD data agrees quite well with that from QNS experiments consistent with the nice agreement of ISF for low Q values between MD simulations and QNS experiments. However l_{jump} and τ_0 parameters from RJD fits to QNS data are systematically higher than those from RJD fits to MD data. This results in a different Q dependence of the translational correlation times discussed below. Rotational relaxation times (τ_{rot}) from QNS experiments are also in satisfactory agreement with those from the RJD model fits to MD simulations.

V. Rotational Diffusion of Water

Anisotropy of Water Rotational Relaxation. Unlike the rotation of a water molecule in bulk water, water motion in poly(vinyl alcohol)/water solutions was found in MD simulations[41] to be strongly anisotropic because of strong hydrogen bonding between water and PVA. As PEO forms hydrogen bonds with water,[16,22] we expect a similar effect to be present in PEO/water solutions. To study water rotational motion in various directions, we define a basis of three vectors uniquely identifying the orientation of a water molecule: (a) a vector (**HH**) connecting the hydrogen atoms, (b) a vector directed along the bisector of the H−O−H bend, corresponding to the direction of the water dipole moment (μ), and (c) a vector perpendicular to the plane of a water molecule ($\perp$ vector). $P_1(t)$ and $P_2(t)$ autocorrelation functions were calculated for relaxation of **HH**, μ, and $\perp$ vectors by

$$P_1(t) = \langle[\mathbf{e}(t)\cdot\mathbf{e}(0)]\rangle \tag{8}$$

$$P_2(t) = 0.5[3\langle[\mathbf{e}(t)\cdot\mathbf{e}(0)]^2\rangle - 1] \tag{9}$$

where $\mathbf{e}(t)$ is a unit vector in the direction of the **HH**, μ, and $\perp$ vectors, t is time, and $\langle\ \rangle$ denotes the ensemble average over all such vectors. Decay of the $P_1(t)$ and $P_2(t)$ autocorrelation functions obtained from MD simulations to 0.01 was approximated by a Kohlrausch−Williams−Watts (KWW) expression given by

$$P_{KWW}(t) = \exp[-(t/\tau)^\beta] \tag{10}$$

Autocorrelation times τ_1 and τ_2 were calculated as time integrals of the KWW fits to $P_1(t)$ and $P_2(t)$ and are shown in Figure 4.

Examination of the temperature dependence of the τ_1 and τ_2 autocorrelation times reveals a slight deviation from Arrhenius behavior at low temperatures, indicative of the coupling of water dynamics to PEO dynamics, as PEO exhibits non-Arrhenius behavior of ISF, dielectric, and torsional relaxation times in PEO/water solutions.[42] Figure 4a shows that the τ_1 correlation time for the dipole vector μ is the longest and the τ_1 correlation time for the vector perpendicular to water plane is the shortest, with the ratio of $\tau_1(\mu)/\tau_1(\perp)$ being about 2.5 at 298 K. Analysis of the τ_2 relaxation times indicates that all relaxation times are similar (within 20%) with τ_2(**HH**) being the longest. Such a

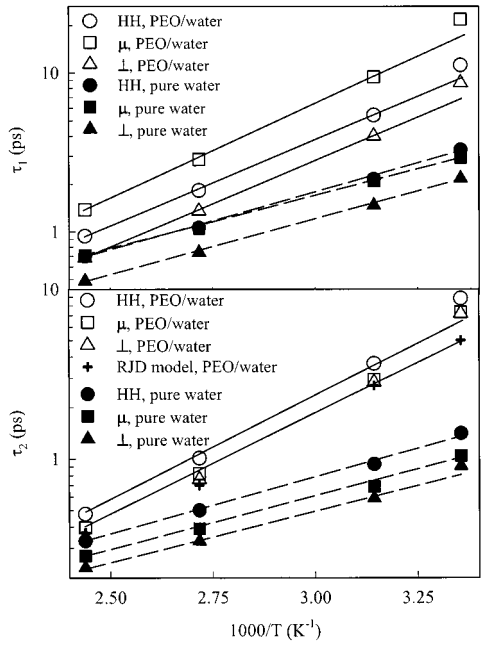

Figure 4. Water rotational relaxation times as a function of temperature from MD simulations and the RJD model analysis for PEO/water solutions (open symbols) and pure water (closed symbols).

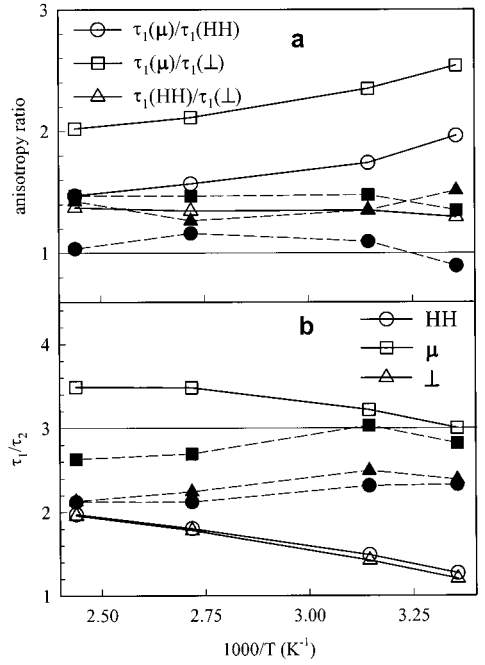

Figure 5. Ratio of τ_1/τ_2 rotational relaxation times (a) and anisotropy ratios (b) as a function of temperature from MD simulations for PEO/water solutions (open symbols) and pure water (closed symbols).

behavior of τ_1 and τ_2 rotational relaxation times indicates that the **HH** and $\perp$ vectors decorrelate (i.e., rotate) much faster than the μ vector. Preferential rotation of water molecules in the plane perpendicular to the μ-vector is consistent with $\tau_1(\mu)$ being significantly larger than τ_1(**HH**) and $\tau_1(\perp)$, whereas the τ_2 values were found to be similar. To further examine water rotational anisotropy, we calculated the ratio of the τ_1 and τ_2 autocorrelation times shown in Figure 5a,b. Figure 5a shows that the anisotropy ratio $\tau_1(\mu)/\tau_1(\perp)$ is the largest, indicating that water tends to rotate in such a way that its μ vector moves much slower than the vector perpendicular to the water plane. This anisotropy ratio is the largest at 298 K and gradually decreases with increasing temperature.

Analysis of τ_1/τ_2 ratio is also helpful in elucidation of the mechanism of water rotation. This ratio is expected to be three for completely isotropic vector rotation, much larger than three for vector rotation on the surface of a cone and much smaller than three for vector rotation in a plane. As $\tau_1(\mu)/\tau_2(\mu)$ is very close to three for the whole temperature range, this implies isotropic motion of the dipole vector. The ratios τ_1(**HH**)/τ_2(**HH**) and $\tau_1(\perp)/\tau_2(\perp)$ drop significantly below three as the temperature decreases, indicative of preferential water rotation in a plane including both the **HH** and $\perp$ vectors. The only plane allowing such motion to occur is the plane perpendicular to the μ vector, in agreement with the previous conclusion of water rotation in the plane perpendicular to μ-vector being much faster than the rotation of the μ vector at low temperatures in PEO/water solutions.

Comparison of RJD Model and MD Simulation Predictions. Rotation of water is commonly described in the analysis of QNS data by the expansion due to Sears[39] (eq 6) based upon the model of random rotation of protons on the surface of a sphere. In our previous studies of TIP4P water and DME/water solutions,[9] we found that for pure water and dilute DME solutions the decay of the rotational component of the ISF is well described by the first three terms of the Sears expansion (eq 6), whereas at a high concentration of DME (DME mole fraction of 0.72), the initial decay of the rotational ISF was adequately described only for small momentum transfers ($Q < 1.3$ Å^{-1}), and significant deviations of the initial decay from the form of eq 6 were observed for $Q > 2$ Å^{-1}. In pure water, the ratio of $\tau_1(\mu)/\tau_1(\perp)$ rotational relaxation times indicating anisotropy of water rotation is close to one for pure water (Figure 5a) suggesting that water rotational dynamics is only slightly anisotropic in pure water. In contrast, water rotational relaxation was found to be more anisotropic at 298 K in PEO/water solutions (Figure 5a), suggesting that water protons do not undergo random motion on the surface of a sphere. Hence, it is reasonable to expect significant deviations of the rotational ISFs from the time dependence of eq 6 at that temperature. On the other hand, the more isotropic rotational relaxation of water at 410 K is expected to yield water proton motion close to the random motion on a surface of a sphere. The rotational ISFs[43] for water in PEO/water solutions at 298, 368, and 410 K from MD simulations together with the fits obtained using eq 6 are shown in Figure 6a−c. Parameters of the fits are shown in Table 1. The fits are the best for small momentum transfers at high temperatures, gradually getting worse with increasing Q and decreasing temperature. This behavior is in accord with water motion being more anisotropic at low temperatures discussed above. Despite the failure of the Sears expansion to describe the initial decay of the rotational ISFs, especially for large momentum transfers, the model still adequately describes the asymptotic long-time behavior of rotational ISFs consistent with the water radius of gyration value of 0.92 Å. The inability of the model to describe the decay of the rotational ISF at 298 K and (to a lesser extent) at 368 and 410 K on the time scale accessible in QNS measurements (i.e., 1−30 ps) brings into serious question the accuracy of the rotational relaxation time τ_{rot} obtained by fitting RJD model to $S(Q,\omega)$.

Comparison of the τ_{rot} obtained by fitting RJD model to the total ISF from MD simulations and τ_{rot} obtained by fitting only the rotational component of ISF from MD simulations with the Sears expansion is shown in Table 1. The values of τ_{rot} obtained by these two approaches differ by a factor of 2−4 casting serious doubt on the possibility of obtaining water rotation from QNS spectra by using RJD model for polymer/water solutions.

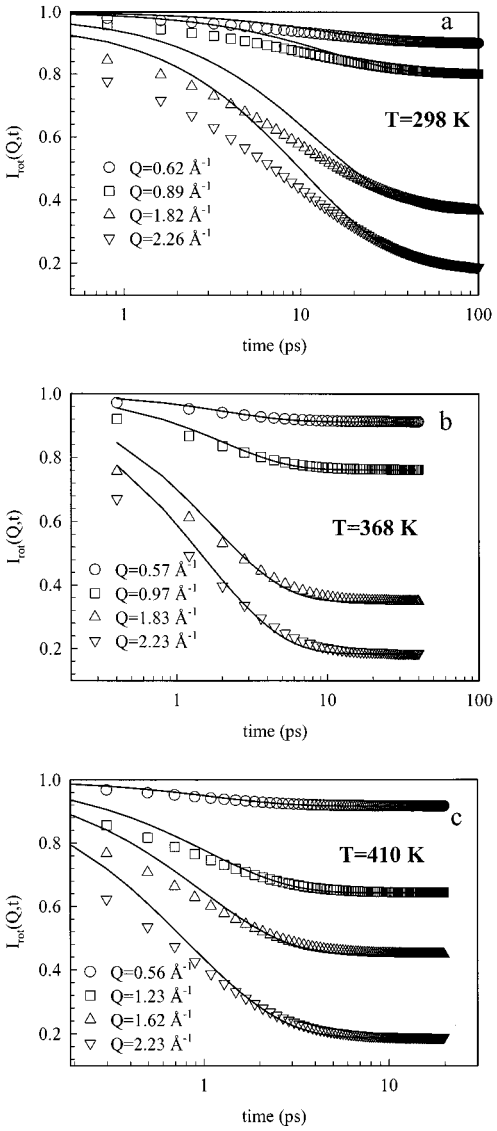

Figure 6. Rotational ISF from MD simulations (open symbols) and fits by eq 6 (lines) for 298 (a), 368 (b), and 410 K (c).

A possible explanation for the smaller τ_{rot} obtained from $I(Q,t)$ fits compared to fits to the rotational component of ISF with Sears expansion could be due to differences in the time window of the fits. The $I(Q,t)$ values were fit in the experimental time window of 0.5−35 ps, whereas $I_{rot}(Q,t)$ were fit from 0.5 to 100 ps to yield correct limiting values of $I_{rot}(Q,t)$. If one only needs to describe a $I_{rot}(Q,t)$ for times up to 30 ps corresponding to the experimental time scale, a smaller value of τ_{rot} will be necessary, consistent with values of τ_{rot} shown in Table 1.

To understand the sensitivity of the total ISF in the RJD model on τ_{rot} parameter, we fit the RJD model to $I(Q,t)$ data from MD simulations with $\tau_{rot} = 4.99$ ps for 298 K and $\tau_{rot} = 0.37$ ps for 410 K, i.e., with τ_{rot} constrained to the value obtained from fitting the Sears expansion to $I_{rot}(Q,t)$. These fits together with the fits where τ_{rot} was allowed to vary are shown in Figure 7a,b for 298 ($\tau_{rot} = 1.35$ ps) and 410 K ($\tau_{rot} = 0.14$ ps), respectively. The fits where τ_{rot} was allowed to vary are slightly better than those with the constrained τ_{rot} to the value obtained from fitting the Sears expansion to $I_{rot}(Q,t)$, but the difference is probably not much greater than the experimental uncertainty of the QNS measurement. It can be seen that changes in the rotational relaxation time of water by a factor of 3 leads to a relatively small changes in $I(Q,t)$.

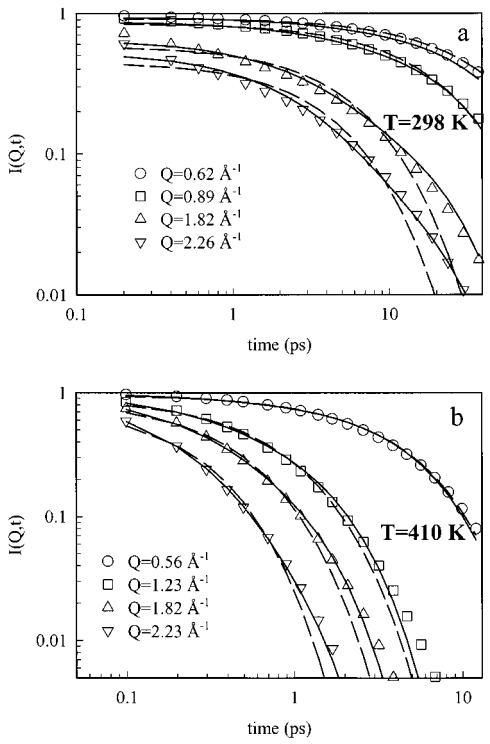

Figure 7. Total ISF ($I(Q,t)$) from MD simulations (symbols) together with RJD fits to $I(Q,t)$ where all parameters were allowed to vary (solid line) and RJD fits where the water rotational constant was constrained to $\tau_{rot} = 4.99$ ps at 298 K and $\tau_{rot} = 0.37$ at 410 K. (dashed line).

VI. Translational Diffusion of Water

Comparison of the RJD Model and MD Simulations. In this section, we investigate the ability of the RJD model to describe translational dynamics obtained from the MD simulations. First, we will check the assumption of the RJD model that the decay of water center of mass ISF ($I_{cm}(Q,t)$) obeys single-exponential behavior on the experimental time scale of 0.5−30 ps, and then we discuss the Q dependence of the inverse correlation time for the translational motion equal in the case of an exponential decay to the translational line width $\Gamma(Q)$.

Figure 8a,b shows $I_{cm}(Q,t)$[44] from MD simulations with the corresponding fits by the RJD model given by eqs 3−5 at 298 and 410 K. $I_{cm}(Q,t)$ can be described as satisfactory for small Q values ($Q < 1.0$ Å) at 298 K, whereas for large Q values, significant deviations of the fit from $I_{cm}(Q,t)$ data are seen. The quality of the fits improves with increasing temperature, with fits at 410 K (Figure 8b) being acceptable. Self-diffusion coefficients obtained from the fits to $I_{cm}(Q,t)$ assuming Gaussian (eq 3−5) behavior are compared in Table 1 with those obtained by fitting $I(Q,t)$ with the RJD model from MD simulations. At 368 and 410 K, the agreement is good, whereas at 298 K, the water self-diffusion coefficient from the $I_{cm}(Q,t)$ fit is about 50% higher than that from the RJD fit to $I(Q,t)$. To determine which of the fits gives more reliable results, we have calculated the water self-diffusion coefficient from mean-square displacements (MSD) using the following relation:[30]

$$D_W = \lim_{t\to\infty} \frac{\langle R_{w(t)}{}^2 \rangle}{6t} \tag{11}$$

where $R_{w(t)}{}^2$ is MSD of a water molecule during time t, and $\langle\ \rangle$ denotes an ensemble average. Table 1 shows that water self-diffusion coefficient from MSD agrees nicely with those

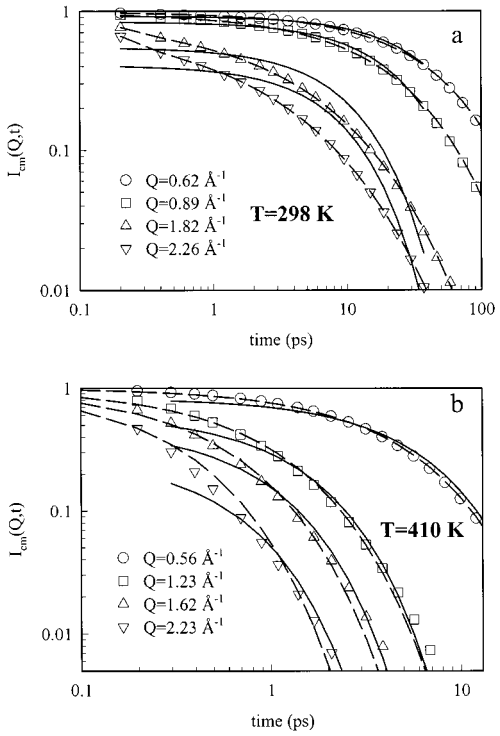

Figure 8. Water center of mass ISF ($I_{cm}(Q,t)$) from MD simulations (symbols), RJD model fits (solid line), and MKWW fits (dashed line).

obtained by fitting $I_{cm}(Q,t)$ with a single-exponential expression despite large deviation of the fits from $I_{cm}(Q,t)$ for low temperatures and high momentum transfers. Good agreement between the water self-diffusion coefficient from MSD and RJD fits to $I(Q,t)$ at 368−410 K also indicates that reliable self-diffusion coefficient could be obtained from RJD fits to QNS data at this temperature range. This supposition does not hold, however, at 298 K where water self-diffusion coefficient from the RJD fit to $I(Q,t)$ is 50% higher than that obtained from MSD, warning that the value of the water self-diffusion coefficient obtain from RJD model fits to QNS could be as large as 50% off the correct value despite of good fit to the data. A possible explanation for this is that, because $I_{cm}(q,t)$ does not follow a single-exponential decay, a larger value of the rotational relaxation time τ_{rot} is needed to make up for the deficiencies of the fits of $I_{cm}(q,t)$ by a single exponent at high Q values; that is, it is needed to make the fits more stretched or KWW-like. An incorrect description of water rotation also leads to incorrect contribution due to water translation at large momentum transfers resulting in a large error in water self-diffusion coefficient. QNS measurements at small momentum transfer values would allow one to overcome this problem, but in this case, no information about water rotation could be obtained.

We proceed by analyzing the Q dependence of the inverse correlation time for the translational motion, which is equal to the translational line width $\Gamma(Q)$ (eq 3) if $I_{cm}(Q,t)$ can be described by a single exponential. The Q dependence of the translational line width $\Gamma(Q)$ of pure water at room temperature and under supercooled conditions has been subject to a controversy.[36,40] RJD analysis of the QNS data on pure water suggested a much more significant flattening of $\Gamma(Q)$ with increasing Q[36] than it was found in MD simulations.[40] The disagreement was especially pronounced at lower temperatures, where a stretched exponential was required to describe the decay of $I_{cm}(Q,t)$.[45]

To calculate the correlation time for the decay of $I_{cm}(Q,t)$ defined as a time integral of $I_{cm}(Q,t)$ from zero to infinity, we

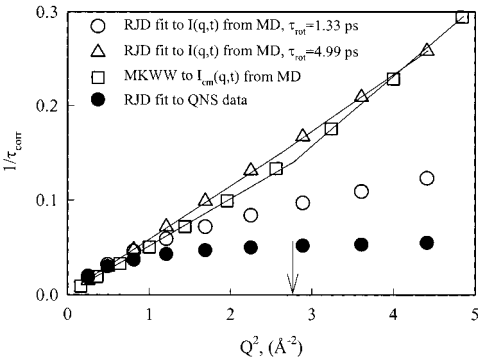

Figure 9. Inverse translational relaxation time from MD simulations together with the RJD model and MKWW fits to QNS data.

approximated $I_{cm}(Q,t)$ with a modified KWW (MKWW) expression following Sciortino et al.:[45]

$$I_{cm}(Q,t) = [1 - A(Q)] \exp[-(t/\tau_s)^2] + A(Q) \exp[-(t/\tau_{long})^{\beta}] \quad (12)$$

The first term in eq 12 describes the processes on the fast time scale, whereas the stretched exponential term describes the slow decay also called α relaxation.[45] Figure 8a,b shows that eq 12 fits the decay of $I_{cm}(Q,t)$ on all time scales nicely, unlike a single-exponential expression (eq 3).

Inverse translational correlation times from the RJD model fits to MD $I(Q,t)$ and QNS $S(Q,\omega)$ data together with the inverse translational relaxation times obtained by integrating MKWW fits to $I_{cm}(Q,t)$ (eq 12) are shown in Figure 9. Inverse relaxation times from the RJD model fits to the QNS data agree the best with the RJD fits to MD $I(Q,t)$ data where all the parameters were allowed to vary, i.e., $\tau_{rot} = 1.33$ ps. Both of these fits, however, deviate significantly from the most accurate inverse translational relaxation times obtained from MKWW fits. Significant deviation of the inverse translational relaxation times obtained by the RJD model fits to $I(Q,t)$ from those from MKWW fits indicate that fitting of the RJD model to $I(Q,t)$ gives incorrect Q dependence of the accurate inverse translational relaxation times. However, if the correct (i.e., yielding correct limiting values of $I_{rot}(Q,t \rightarrow \infty)$, $\tau_{rot} = 4.99$ ps) rotational relaxation time is used for fitting the RJD model to $I(Q,t)$ values, a much better agreement with MKWW fits could be obtained.

Further examination of the Q dependence of the inverse translational relaxation times from MKWW fits indicates that a change of slope takes place at about 1.6 Å^{-1}, indicating that water is caged between PEO in accord with the previous QNS analysis of PEO/water solutions.[24,25] A more detailed discussion of the water caging is given in the next paper dealing with concentration dependence of water dynamics[46] in PEO/water solutions.

VII. Influence of PEO on Water Relaxation

According to our MD simulations, the water rotational relaxation times at 298 K increase about half an order of magnitude for τ_1(**HH**) and $\tau_1(\perp)$ and almost an order of magnitude for $\tau_1(\mu)$ compared to water rotation in bulk water (Figures 4 and 10). This indicates that addition of PEO slows down water μ vector reorientation more dramatically than **HH** and $\perp$ vector reorientation leading to a higher anisotropy of water rotation in PEO/water compared to pure water especially at low temperatures (Figure 5). It is reasonable to suggest that water−PEO dipole−dipole interactions shown in Figure 11 are responsible for such behavior, as it would inhibit μ vector motion

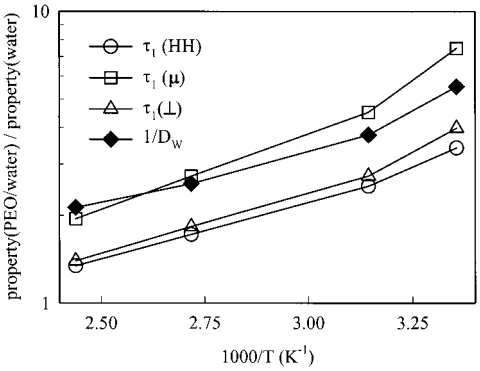

Figure 10. Ratio of the rotational and translational characteristic relaxation times of water in PEO/water solutions at $w_P = 0.52$ to that in pure water from MD simulations.

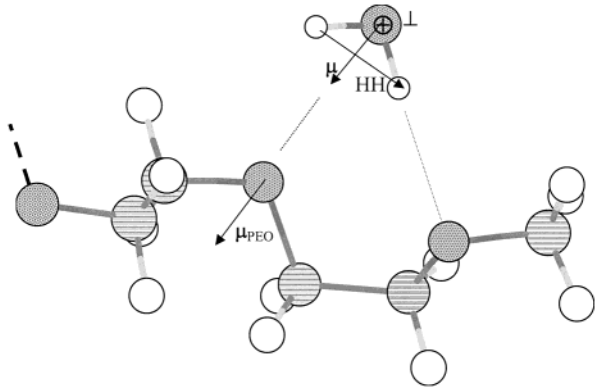

Figure 11. Schematic picture of water−PEO favorable dipole−dipole interactions and hydrogen bonding.

to a greater extent than the motion of **HH** and ⊥ vectors. Increasing temperature leads to a decrease in the difference between water rotational dynamics in PEO/water solutions and in bulk water. An especially dramatic decrease is observed for the μ vector rotation relaxation time. This coincides remarkably well with a decrease in PEO−water hydrogen bonding[16] and a decrease of the fraction of the PEO conformers[15] with favorable PEO−water dipole−dipole interactions with increasing temperature. At 410 K, water rotational relaxation times in PEO/water solutions are within a factor of 2 from those in the bulk water, suggesting that at that temperature PEO−water interactions are weak enough that water exhibits rotational dynamics quite similar to that of bulk water. This weakening of PEO−water interactions with increasing temperature could be potentially responsible for PEO−water phase separation at higher temperatures.[47]

Examination of the temperature dependence of the characteristic translational time of water in PEO/water solutions given as $(1/D_W)$ relative to that in pure water reveals a decrease in $[1/D_w(\text{PEO/water})]/[1/D_w(\text{pure water})]$ with increasing temperature as seen for the analogous ratio of the rotational relaxation times. The rate of this decrease is similar to that observed for $\tau_1(\mu)$ but larger than that for $\tau_1(\text{HH})$ and $\tau_1(\perp)$, indicating coupling between mechanisms of water dipole moment vector rotation and water diffusion in PEO/water solutions.

VIII. Conclusions

Water rotational and translational diffusion were investigated in a joint MD simulation and QNS experimental study of PEO/water solutions in the temperature range of 298−410 K. The water self-diffusion coefficient and the intermediate scattering functions from MD simulations are in good agreement with those from QNS experiments at small momentum transfers, supporting the validity of the quantum-chemistry-based PEO/water force field used in the MD simulations.

Despite of the ability of the RJD model to adequately fit $S(Q,\omega)$ QNS data and $I(Q,t)$ MD simulations data at 298 K, MD simulations indicate that the water self-diffusion coefficient from the RJD fit to $I(Q,t)$ is about 50% higher than that extracted from the mean-square displacements and rotational relaxation time is smaller by a factor of 3 from that extracted directly from the rotational ISFs. At higher temperatures (368 and 410 K), MD simulations indicate good agreement between the self-diffusion coefficient from the RJD fit to $I(Q,t)$ and that extracted from the mean-square displacements; however, the rotational relaxation time from the RJD fit to $I(Q,t)$ is still 2.5−4 times smaller from that extracted from the rotational ISFs. Thus, one needs to interpret parameters of RJD fits to QNS data of polymer/water solutions with caution especially at low temperature.

The Sears expansion for $I_{rot}(Q,t)$ assuming rotation of water protons on a surface of the sphere was found to properly describe long time values of $I_{rot}(Q,t\rightarrow\infty)$, but initial decay at large momentum transfers and low temperatures of $I_{rot}(Q,t)$ cannot be described by Sears expansion because of anisotropy of water rotational motion. Water was found to have preferential rotation around its dipole moment vector due to electrostatic interactions with PEO. This effect is especially pronounced at low temperatures where the most extensive PEO−water hydrogen bonding was observed.

Finally, the dipole vector rotational autocorrelation time and the water self-diffusion coefficient are significantly changed upon water complexation with PEO molecules compared to the values in pure water, whereas $\tau_1(\text{HH})$ and $\tau_1(\perp)$ rotational autocorrelation times are much less affected by the addition of PEO to water. The difference between water rotational and translational relaxation in PEO/water and in bulk water decreases with increasing temperature.

Acknowledgment. The authors are indebted to the National Science Foundation, Division of Materials Research, for support provided through the NSF award DMR 0076306. An allocation of computer time from the Center for High Performance Computing at the University of Utah is gratefully acknowledged. CHPC's IBM SP system is funded in part by NSF Grant No. CDA9601580 and IBM's SUR grant to the University of Utah. This work was supported by the U.S. Department of Energy and funded in part by its Office of Science, Office of Basic Energy Sciences under Contract W-7405-ENG-36 at Los Alamos National Laboratory and Contract W-31-109-ENG-38 at Argonne National Laboratory.

References and Notes

(1) Amiji, M.; Park, K. *Biomaterials* **1992**, *13*, 682.
(2) Jeon, S. I.; Lee, J. H.; Andrade, J. D.; de Gennes, P. G. *J. Colloid Interface Sci.* **1991**, *142*, 129.
(3) Harris, J. M. *Poly(Ethylene Glycol) Chemistry. Biotechnical and Biomedical Applications*; Plenum Press: New York, 1992.
(4) Harris, J. M.; Zalipsky, S. *Poly(Ethylene Glycol): Chemistry and Biological Applications*; ACS Symposium Series, No. 680; American Chemical Society: Washington, DC, 1998.
(5) Morra, M.; Occhiello, E.; Garbassi, F. *Clin. Mater.* **1993**, *14*, 255.
(6) Espadas-Torre, C.; Meyerhoff, M. E. *Anal. Chem.* **1995**, *67*, 3108.
(7) Cappello, B.; Del Nobile, M. A.; La Rotonda, M. I.; Mensitieri, G.; Miro, A.; Nicolais, L. *Il Parmaco* **1994**, *49*, 809.
(8) Bedrov, D.; Pekny, M.; Smith, G. D. *J. Phys. Chem. B* **1998**, *102*, 996.
(9) Trouw, F.; Bedrov, D.; Borodin, O.; Smith, G. D. *Chem. Phys.* **2000**, *261*, 137.

(10) Bedrov, D.; Borodin, O.; Smith, G. D. *J. Phys. Chem. B* **1998**, *102*, 5683.
(11) Bedrov, D.; Borodin, O.; Smith, G. D. *J. Phys. Chem. B* **1998**, *102*, 9565.
(12) Borodin, O.; Bedrov, D.; Smith, G. D. *Macromolecules* **2001**, *34*, 5687.
(13) Bedrov, D.; Smith, G. D. *J. Phys. Chem. B* **1999**, *103*, 3791.
(14) Bedrov, D.; Borodin, O.; Smith, G. D.; Trouw, F.; Mayne, C. *J. Phys. Chem. B* **2000**, *104*, 5151.
(15) Smith, G. D.; Bedrov, D.; Borodin, O. *J. Am. Chem. Soc.* **2000**, *122*, 9548.
(16) Smith, G. D.; Bedrov, D.; Borodin, O. *Phys. Rev. Lett.* **2000**, *85*, 5583.
(17) Liu, H.; Müller-Plathe, F.; van Gunsteren, W. F. *J. Chem. Phys.* **1995**, *102*, 1722.
(18) Engkvist, O.; Åstrand, P.; Karlström, G. *J. Phys. Chem.* **1996**, *100*, 6950.
(19) Williams, D. J.; Hall, K. B. *J. Phys. Chem.* **1996**, *100*, 8224.
(20) Tasaki, K. *J. Am. Chem. Soc.* **1996**, *118*, 8459.
(21) Engkvist, O.; Karlström, G. *J. Chem. Phys.* **1997**, *106*, 2411.
(22) Smith, G. D.; Borodin, O.; Bedrov, D. *J. Comput. Chem.* Submitted for publication.
(23) Barnes, A. C.; Bieze, T. W.; Enderby, J. E.; Leyte, J. C. *J. Phys. Chem.* **1994**, *98*, 11527.
(24) Crupi, V.; Jannelli, M. P.; Magazu, S.; Maisna, G.; Majolino, D.; Migliardo, P.; Vasi, C. *Il Nuovo Cimento* **1994**, *16*, 809.
(25) Crupi, V.; Magazu, S.; G.; Majolino, D.; Migliardo, P.; Wanderlingh, U.; Kagunya, W. W. *Physica B* **1998**, *241*−*243*, 979.
(26) Bradley, K. F.; Chen, S.-H.; Brun, T. O.; Kleb, R.; Loomis, W. A.; Newsam, J. M. *Nucl. Instr. Methods* **1988**, *A270*, 78.
(27) Smith, G. D.; Jaffe, R. L.; Yoon, D. Y. *J. Phys. Chem.* **1993**, *97*, 12752.
(28) Jorgensen, W. L.; Chandrasekhar, J.; Madura, J. D.; Impey, R. W.; Klein, M. *J. Chem. Phys.* **1983**, *79*, 926.
(29) Smith, G. D.; Jaffe, R. L.; Yoon, D. Y. *Macromolecules* **1993**, *26*, 298.
(30) Allen, M. P.; Tildesley, D. J. *Computer Simulation of Liquids*; Oxford University Press: New York, 1987.
(31) Nose, S. In *Computer Simulation in Materials Science*; Meyer, M., Pontikis, V., Eds.; Kluwer Academic Publishers: Norwell, MA, 1991; p 21.
(32) Martyna, G. J.; Tuckerman, M.; Tobias, D. J.; Klein, M. L. *Mol. Phys.* **1996**, *87*, 1117.
(33) Ryckaert, J. P.; Ciccotti, G.; Berendsen, H. J. C. *J. Comput. Phys.* **1977**, *23*, 327.
(34) Kittel, C. *Introduction to the Theory of Solids*, 2nd ed; Wiley: New York, 1956; Appendix A.
(35) Higgins, J. S.; Benoît, H. C. *Polymers and Neutron Scattering*; Clarendon Press: Oxford, U.K., 1996.
(36) Teixeira, J.; Bellisent-Funel, M. C.; Chen, S. H.; Dianoux, A. J. *Phys. Rev.* **1985**, *A31*, 1913.
(37) Bellissent-Funel, M.-C.; Zanotti, J.-M.; Chen, S. H. *Faraday Discuss.* **1996**, *103*, 281.
(38) Singwi, K. S.; Sjölander, A. *Phys. Rev.* **1960**, *119*, 863.
(39) Sears, W. F. *Can. J. Phys.* **1966**, *44*, 1299.
(40) Ullo, J. J. *Phys. Rev. A* **1987**, *36*, 816.
(41) Müller-Plathe, F. *J. Chem. Phys.* **1998**, *108*, 8252.
(42) Borodin, O.; Bedrov, D.; Smith, G. D. *Macromolecules* **2001**, *34*, 5687.
(43) $I_{rot}(Q,t) = \langle[\sin(\Delta R_i(t)Q)]/[\Delta R_i(t)Q]\rangle$, where $\Delta R_i(t)$ is the displacement of the vector connecting atom *i* with the center of mass of the molecule containing atom *i* after time *t*, *Q* is the magnitude of the momentum transfer vector, and $\langle\ \rangle$ denotes an average over all time origins.
(44) $I_{cm}(Q,t) = \langle[\sin(\Delta r_i^{cm}(t)Q)/\Delta r_i^{cm}(t)Q\rangle$, where $\Delta r_i^{cm}(t)$ is the displacement the center of mass of the molecule *i* after time *t*, *Q* is the magnitude of the momentum transfer vector, and $\langle\ \rangle$ denotes an average over all time origins.
(45) Sciortino, F.; Gallo, P.; Tartaglia, P.; Chen, S.-H. *Phys. Rev. E* **1996**, *54*, 6331.
(46) Borodin, O.; Bedrov, D.; Smith, G. D. *J. Phys. Chem. B* **2002**, *106*, 5194.
(47) Saeki, S.; Kuwahara, N.; Nakata, M.; Kaneko, M. *Polymer* **1976**, *17*, 685.